



HHS Public Access

Author manuscript

Acta Biomater. Author manuscript; available in PMC 2019 March 15.

Published in final edited form as:

Acta Biomater. 2018 March 15; 69: 313–322. doi:10.1016/j.actbio.2018.01.033.

Introduction of sacrificial bonds to hydrogels to increase defect tolerance during suturing of multilayer vascular grafts

Allison Post, M.S.¹, Alysha P. Kishan, Ph.D.¹, Patricia Diaz-Rodriguez, Ph.D.², Egemen Tuzun, M.D.³, Mariah Hahn, Ph.D.², and Elizabeth Cosgriff-Hernandez, Ph.D.⁴

¹Department of Biomedical Engineering, Texas A&M University, College Station, Texas, 77843

²Department of Biomedical Engineering, Rensselaer Polytechnic Institute, Troy, New York 12180

³Texas A&M, Institute for Preclinical Studies, Texas A& M University, 800 Raymond Stotzer, College Station, Texas 77843

⁴Department of Biomedical Engineering, University of Texas, Austin, Texas, 78712

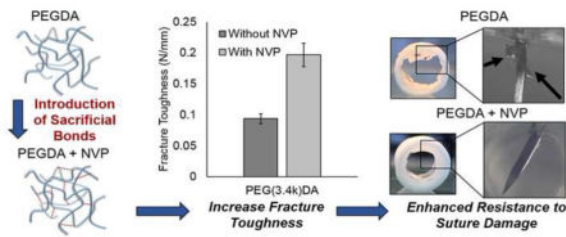
Abstract

Small-caliber vascular grafts used in coronary artery bypass procedures typically fail due to the development of intimal hyperplasia or thrombosis. Our laboratory has developed a multilayered vascular graft with an electrospun polyurethane outer layer with improved compliance matching and a hydrogel inner layer that is both thromboresistant and promotes endothelialization. Initial *in vivo* studies showed that hydrogel particulates were dislodged from the hydrogel layer of the grafts during suturing. To address this problem, we developed and characterized a new hydrogel formulation that resists damage during suturing. Introduction of sacrificial, hydrogen bonds to poly(ethylene glycol)-based hydrogels via co-polymerization with n-vinyl pyrrolidone (NVP) increased the fracture energy as determined by single edge notch testing. This enhanced defect tolerance resulted in a hydrogel layer that was resistant to suture-induced damage with no dislodged particles observed. Importantly, the incorporation of NVP did not affect the thromboresistance, bioactivity, or biostability of the hydrogel layer. In addition to eliminating complications due to hydrogel particle generation in our multilayer graft design, this defect tolerant hydrogel formulation has broad potential use in many cardiovascular and soft tissue applications.

Graphical Abstract

[†]Corresponding author address: 107 W. Dean Keaton, BME 3.503D, 1 University Station, C0800, Austin, TX 78712, Tel: (512) 471-7679, Fax: (512) 471-0616, cosgriff.hernandez@utexas.edu.

Publisher's Disclaimer: This is a PDF file of an unedited manuscript that has been accepted for publication. As a service to our customers we are providing this early version of the manuscript. The manuscript will undergo copyediting, typesetting, and review of the resulting proof before it is published in its final citable form. Please note that during the production process errors may be discovered which could affect the content, and all legal disclaimers that apply to the journal pertain.



Keywords

hydrogel; suture damage resistance; sacrificial bonds; vascular graft; thromboresistant coating

INTRODUCTION

There remains a critical need for improved vascular prostheses in small-caliber applications such as coronary artery bypass surgeries. Current synthetic vascular grafts are fraught with problems that lead to poor 5-year patency rates.[1, 2] Given that platelet aggregation and smooth muscle cell proliferation may be mediated by promoting endothelial cell and endothelial progenitor cell adhesion and migration, the development of materials that direct appropriate cell behavior would have a significant impact on small vessel repair and replacement.[3, 4] In order to circumvent the time and cost associated with cell harvesting and extended pre-culture, researchers have focused on the development of biomaterials that are both thromboresistant and promote post-implantation endothelialization.[5] However, matrix properties that promote graft endothelialization may not be consistent with those appropriate to sustain the loads associated with adult vasculature. To address this limitation, we have developed multilayered conduits comprised of a hydrogel layer designed to induce rapid endothelialization and a reinforcing mesh sleeve designed to provide bulk strength, compliance matching, and suture retention.[5] Thus, each component can be individually tuned to achieve improved outcomes without detriment to other design goals and then bonded together into composite grafts. The fabrication of this multilayered graft is depicted in Figure 1A. An electrospun polyurethane outer layer is placed into a custom mold with a glass mandrel in the center, a hydrogel precursor solution is pipetted between the graft and the mandrel, and the hydrogel layer was photopolymerized with UV light to generate a multilayer composite.

Our preliminary research demonstrates that we can achieve multilayer constructs with clinically relevant mechanical properties that also display acute thromboresistance, controlled endothelial cell migration, and biostability.[5–7] After implantation as end-to-end anastomosis into the carotid arteries of 6 month old swine, damage to the hydrogel coating of the composite graft was observed, as demonstrated in Figure 1B. The generation of hydrogel particulates during suturing of the grafts represents a significant risk that must be addressed prior to further graft development and assessment. The risks associated with dislodged hydrogel particulates are similar to those of a thrombus or embolus and include stroke, heart attack, and pulmonary embolism.[8] There is a clear need for a hydrogel coating in the multi-layered small diameter vascular graft that does not generate particulates

after suturing that can act as emboli downstream. However, no suture damage resistant hydrogels or requisite material properties have been described in literature to the best of our knowledge. We also found that common mechanical properties evaluated in hydrogels such as compressive and tensile modulus, toughness, and elongation did not correlate to particles dislodged during suturing. Due to the lack of hydrogels exhibiting suture damage resistance, we have developed a hydrogel to address this need.

In order to resist suture damage, the hydrogel must be resistant to crack propagation initiated by passing a suture needle through it. This can be accomplished by increasing the energy required to initiate crack propagation by increasing the secondary force interactions between adjacent polymer chains.[9] Enhancing secondary bonding or sacrificial bonds increases the energy required to initiate crack propagation through a material. Therefore, increasing hydrogen bonding can increase the defect tolerance in the hydrogel coating. We hypothesize that by introducing increased hydrogen bonding in the hydrogel, crack propagation and the associated dislodged particles will decrease. To this end, we enhanced hydrogen bonding by incorporating n-vinyl pyrrolidone (NVP) into the hydrogel to create a clinically relevant graft.

A PEG-based hydrogel with enhanced hydrogen bonding was developed to prevent damage to the hydrogel coating during suturing of our vascular graft. Initially, the mechanical properties of several hydrogel formulations were investigated to identify the impact of hydrogen bonding and correlation to suture-induced damage. The hydrogel formulation with the fewest dislodged particles was then evaluated to confirm retention of thromboresistance, bioactivity, and biostability as compared to traditional poly(ethylene glycol) diacrylate (PEGDA) hydrogels. Finally, composite grafts were sutured into excised porcine carotid arteries and hydrogel particulate generation was evaluated in an ex vivo model under physiological flow. This study provides a comprehensive evaluation of this new hydrogel as a vascular graft coating that prevents complications associated with suture-induced particulate generation.

MATERIALS AND METHODS

Materials

Bionate® Thermoplastic Polycarbonate-urethane was provided by DSM Biomedical (Berkeley, CA). All other chemicals were purchased from Sigma Aldrich (Milwaukee, WI) and used as received unless otherwise noted.

PEGDA and PEGDAA Synthesis

Polyethylene glycol diacrylate (PEGDA) was synthesized according to a method adapted from Hahn, et al.[10] Briefly, acryloyl chloride (4 molar equivalents) was added dropwise to a solution of PEG diol (3.4 kDa; 1 molar equivalent) and triethylamine (TEA, 2 molar equivalents) in anhydrous dichloromethane (DCM) under nitrogen. The reaction was stirred for 24 hours, and then washed with 2M potassium bicarbonate (8 molar equivalents). After drying with anhydrous sodium sulfate, the product was precipitated in cold diethyl ether, vacuum filtered, and dried under vacuum. Polyethylene glycol diacrylamide (PEGDAA) was

prepared using a similar method to PEGDA. Briefly, acryloyl chloride was added to a solution of PEG diamine (3.4 kDa) and TEA in anhydrous DCM under nitrogen. The molar equivalent of PEG diamine, TEA, and acryloyl chloride was kept at 1:2:4. After reacting for 24 hours, the solution was similarly washed, precipitated, and dried to obtain the final product. The chemical structures are shown in Figure 2.

Hydrogel fabrication and characterization

Several hydrogel compositional variables were tested including the effect of polymer backbone (PEGDA, PEGDAA), molecular weight (10kDa, 6kDa, 3.4kDa), crosslinker (NVP, 4-arm PEG acrylate), and polymer concentration (3.6, 7.2, 10, 20, 30%). As a generalized fabrication method, hydrogel slabs were fabricated by dissolving PEGDA or PEGDAA in deionized water with 1 vol% of the photoinitiator Irgacure 2595 (10mg/ml in 70% ethanol). NVP was incorporated in select precursor solutions at the molar ratios 1:12, 1:24, or 1:54 of PEG:NVP. Samples containing 4-arm PEG-acrylate were prepared with 10% or 20% 4-arm PEG-acrylate added to the 10% precursor solution of PEGDA. Precursor solutions were mixed and pipetted between 1.5 mm glass spacer plates and crosslinked on a UV plate, 6 minutes on each side.

The sol fraction and swelling ratio was determined for each hydrogel composition ($n = 6$). Briefly, circular hydrogel specimens ($D = 8$ mm) were dried under vacuum immediately after fabrication and weighed (W_d). Specimens were weighed after swelling in deionized water for 24 h (W_s), and then weighed again after drying under vacuum for 24 h to assess dry polymer mass (W_d). The sol fraction was calculated as $(W_s - W_d)/W_s$. The equilibrium volumetric swelling ratio, Q , was calculated from the equilibrium mass swelling ratio: $(W_s)/W_d$.

NVP incorporation

An assay developed by El-Rabbat et al. was used to measure the quantity NVP leached out of the hydrogels as an indirect method to determine NVP incorporation into the polymer network.[11] Briefly, 8 mm hydrogel punches ($n = 6$) were soaked for 3 days with daily solution changes to remove unincorporated NVP. The supernatant was frozen, lyophilized, and re-suspended in 1 ml of glacial acetic acid. NVP was diluted in acetic acid to create the calibration curve. Malonic acid was dissolved at 10 wt% in acetic anhydride at 80°C for 5 minutes to create the working reagent. The working reagent was then added in equal volumes to the re-suspended hydrogel extracts and calibration solutions. The solutions were allowed to stand for 20 minutes at 80°C and then fluorescence read on a plate reader with excitation/emission at 397nm/452nm. The amount of NVP leached out of the gels was calculated using the calibration curve.

Hydrogel mechanical testing

Mechanical testing was performed to determine the effect of compositional variables on the compressive and tensile properties of the hydrogels as well as crack propagation using a single edge notch test. Hydrogels of each composition were fabricated as described above. Compressive modulus was determined using a dynamic mechanical analyzer (DMA) (RSAIII, TA Instruments). Six 8-mm diameter discs were punched from swollen hydrogel

sheets and subjected to mechanical testing using the DMA fitted with a parallel-plate compression clamp. Testing was performed under unconstrained compression at room temperature. Dynamic strain sweeps were used to determine the linear viscoelastic range for each hydrogel formulation. Then, a strain within the upper end of the linear viscoelastic range was used in a constant strain frequency sweep. Tests were conducted between 0.79 and 79 Hz, and the compressive storage modulus was taken at 1.25 Hz.

Tensile testing was performed on hydrogel rings that were fabricated by pipetting the precursor solution into a custom mold with a 3 mm inner diameter and a 5 mm outer diameter. The hydrogel tubes were swollen in deionized water for 24 h and then cut into 3 mm sections. Ring specimens ($n = 6$) were loaded in tension on an Instron 3324, and the stress and strain were recorded as the rings were pulled at a rate of 6 mm/min until failure. Tensile modulus was determined by the slope of the linear region of the stress-strain curve. Ultimate elongation was measured by the stretched length over the original length as a percent, or $(L/L_0)*100$. Ultimate tensile strength was determined as the force at failure. Toughness was measured as the area under the stress-strain curve.

To determine the fracture toughness of the hydrogel compositions, hydrogel specimens were fabricated (30 mm long, 10 mm wide, 1.5 mm thick) for single edge notch mechanical testing. Hydrogels fabricated with PEG(10k)DA, PEG(6k)DA, and PEG(3.4k)DA, each with and without NVP, were tested ($n = 6$). Using a razor blade, a notch 5 mm long was cut halfway along the length of the gel. The gels were then loaded into tensile grips of the RSAIII DMA using sandpaper to prevent hydrogel slippage. The gels were pulled in tension at 1 mm/s until the crack had propagated across the gel. The force of crack propagation was recorded and fracture toughness of the gel was calculated by the force over the length of the crack, $G = 2F/h_0$.

Suture-induced damage in hydrogels

Suture-induced damage was determined by the number of particulates dislodged during the pass of a suture needle and thread through a hydrogel slab. Hydrogel slabs were fabricated as described above and soaked in deionized water for 12 h. A 7-0 suture (Ethicon) was passed through the hydrogel to assess the suture-induced damage. Dislodged hydrogel particles were visualized and counted under a stereoscope (National Optical) as a measure of suture-induced damage of the hydrogel.

Bovine aortic endothelial cell (BAEC) adhesion to hydrogels

Bioactivity was conferred to the hydrogels by adding 4 mg/ml of collagen functionalized with acrylate-PEG-NHS linker (JenKem) (functionalization of 10% of the available lysines) to the 10% PEG(3.4k)DA and 20% PEG(3.4k)DAA-NVP hydrogel precursor solutions prior to cure. The hydrogels were soaked for 3 days prior to cell seeding to remove any uncrosslinked NVP. Circular specimens ($D = 10$ mm) were punched from hydrogel slabs and placed into a 48 well plate. Bovine aortic endothelial cells (BAECs) were cultured in EGM-2 cell media (Lonza), harvested for use at passage P4-P6, and seeded at 10,000 cells per well. Cells were allowed to attach for 3 hours, then washed twice with warm 10 mM phosphate buffered saline (PBS). Specimens were then fixed with 3.7% glutaraldehyde and stained

with rhodamine phalloidin (actin/cytoskeleton) and SYBR green (DNA/nucleus). Cell adhesion and spreading were quantified using ImageJ software (n = 4).

Platelet attachment to hydrogels

Platelet attachment was used as an initial measure of thromboresistance of the new hydrogel formulations. 10% PEG(3.4k)DA and 20% PEG(3.4k)DAA-NVP hydrogels were soaked for 3 days prior to cell seeding to remove any uncrosslinked NVP. Circular hydrogel specimens were punched from the hydrogel slabs and placed in a 48 well plate. Platelets were isolated from human whole blood drawn from a volunteer and mixed with ACD via inversion. The mixture was centrifuged at 990 rpm for 15 minutes to isolate the protein rich plasma (PRP) layer. The PRP layer was removed and prostacyclin was added at 10 $\mu\text{L}/\text{mL}$ and centrifuged again at 1500 rpm for 10 min to form a platelet pellet. The pellet was resuspended in CGS buffer for washing and centrifuged again at 1500 rpm for 10 min. The platelets were then resuspended in Tyrode's buffer at half the original volume of PRP. Sudan B Black solution (5% in 70% ethanol) was added to the platelet solution at a 1:10 ratio for 30 minutes at room temperature. The stained platelets were then washed with PBS 3 times by resuspending the pellet in PBS then centrifuging at 1500 rpm for 8 min. Platelets were counted and resuspended at a concentration of 10×10^6 platelets/mL in sterile PBS. 500 μL platelet suspension was added in each test well, and platelets were allowed to adhere to substrate for 30 min at 37°C on a shaking incubator. Gels were transferred to new wells and washed twice with PBS, then carefully placed into microcentrifuge tubes and bound cells were lysed with 150 μL DMSO for 15 min at room temperature. 150 μL of PBS was added to each sample and the solution moved to a cuvette for reading on a spectrophotometer (400–650 nm, SpectraMax M2, Molecular Devices).

Fabrication of multilayer vascular graft composites

A 25 wt% solution of Bionate® (DSM) in dimethylacetamide was electrospun with a flow rate of 0.5 ml/hr through a blunted 20G needle. The rotating mandrel for collection was coated in a PEG sacrificial layer and placed 50 cm from the needle tip. A voltage of 15 kV was applied to the needle and a -5kV voltage was applied to the rotating mandrel. The rod and mesh were allowed to soak for 1 hour in water to dissolve out the sacrificial PEG layer, and the mesh sleeve was cut into 4 mm long sections. Electrospun mesh sleeves were then taken through a graded ethanol/water soak (70%, 50%, 30%, and 0%; 30 minutes each) to ensure hydration and penetration of the aqueous hydrogel precursor solutions into the mesh prior to hydrogel coating. The pre-wetted meshes were then placed in a cylindrical mold with an inner glass mandrel (3 mm OD). Hydrogel solutions were pipetted between the mandrel and the hydrated mesh (4 mm ID) and crosslinked with UV light for 6 minutes in a custom-built UV box.

Accelerated hydrolytic degradation of hydrogel coatings

Hydrolytic degradations of the hydrogels were first compared in accelerated degradation conditions of 50 mM NaOH at 37°C. 8 mm punches were taken from hydrogel slabs after swelling overnight and put under vacuum overnight. Dry weights were recorded, and the hydrogel punches were swollen in water for 1 hour before weighing to determine the swelling ratio. The gels were then transferred to their respective conditions. Swelling ratio

(Q) was calculated as W_s/W_d . Swollen weights were measured once a day for accelerated degradation of 10% PEG(3.4k)DA, and PEG(3.4k)DAA conditions were measured once a week. Compressive modulus was also recorded at these time points, as described previously.

To evaluate the hydrolytic degradation resistance of the vascular graft composites, multilayer vascular grafts were fabricated with either PEG(3.4k)DAA-NVP or PEG(3.4k)DA precursor solution. The composites were cut into 1cm long sections and incubated in the conditions described above for accelerated hydrolytic degradation. Degradation was measured as a change in luminal diameter. Pictures of the luminal diameter were acquired using a stereoscope (National Optical) and the diameter was measured using ImageJ software.

Bioreactor whole blood study of platelet adhesion of multilayer grafts

The thromboresistance of the multilayer graft was assessed by flowing fresh, heparinized porcine whole blood (Lampire Biological Laboratories) through the lumen of the grafts for extended time periods in a bioreactor. Multilayer grafts with PEGDA or PEG-NVP hydrogel luminal layers (n = 4 per formulation) were fitted onto the graft ports of custom bioreactor graft chambers and fixed into place using sterile nylon thread. Segments of an ePTFE vascular graft control (GORE-TEX® Stretch Vascular Graft ST04015A) were fitted onto remaining graft ports (n = 4). Prior to the onset of flow, the blood was exposed to 10 μ M mepacrine for 30 minutes at 37°C to fluorescently label associated platelets. Samples were perfused with heparinized porcine whole blood for three hours at a flow rate of 100 ml/min/construct generated by a peristaltic pump (Masterflex L/S 07528-30). Grafts were then dismantled from the graft ports and gently rinsed twice with PBS followed by exposure to 10% neutral-buffered formalin. Subsequently, the constructs were cut into two halves using fine-tipped surgical scissors, with the dissection plane slicing the length of each graft. Half of each construct was allocated for fluorescence imaging of adherent platelets, and the remaining half was processed for quantitative assessment of platelet adhesion to the graft lumen. Fluorescence images of platelet adhesion were obtained utilizing a Zeiss Axiovert 200M microscope with a FITC filter set (ex/em 470nm/515nm) and a 20X objective. To quantitatively assess platelet adhesion, the lumen of graft sections were rinsed 3 times with 200 μ L of lysis buffer (100 mM TRIZMA-Base, 500 mM LiCl, 10 mM EDTA, 1% LiDS, 5 mM dithiothreitol). This lysis buffer was collected and associated mepacrine was measured spectrophotometrically (Biotek Synergy HTX plate reader) utilizing a FITC filter set. Sample concentrations were determined relative to a standard curve and then normalized to the luminal surface area of the processed graft section.

Hydrogel particulate capture after suturing composites in ex vivo model

Vascular graft composites, fabricated as described above, were made with either PEG(3.4k)DAA-NVP or PEG(3.4k)DA precursor solution (n = 4). Porcine carotid arteries were acquired from Lampire Biological Laboratories (Pipersville, PA) and used within 48 hours of harvest. The arteries were cleaned and sectioned to 2 cm lengths and sutured to each end of the grafts. Sham suturing was performed by suturing two carotid artery sections together using 7-0 proline sutures with a tapered needle (Ethicon). The sutured grafts and sham were then placed in a flow loop under physiological pressures (80 mmHg to 120 mmHg) for 30 minutes to further dislodge any hydrogel particulates created during suturing.

The flow buffer was collected and filtered for particulates 200 μ m or larger that were then counted manually. The remaining unfiltered particulates were counted using a Chemtrac particle counter (Atlanta, GA). Grafts were then sectioned to visually inspect suture line damage.

Statistical analysis

The data are displayed as mean \pm standard deviation for all measurements with the exception of cell adhesion that is presented as mean \pm standard error of the mean. An analysis of variance (ANOVA) comparison was used for multiple composition comparisons with a Tukey's multiple comparison test to analyze the significance of the data. Comparisons in which there are only two compositions were compared using a student's t-test. Linear trends were tested by determining if the slopes of the best fit lines were statistically non-zero using the linear regression function of GraphPad. All tests were carried out at a 95% confidence interval ($p < 0.05$).

RESULTS

Suture-induced damage in hydrogels

Several hydrogel compositional variables were tested, molecular weight (10kDa, 6kDa, 3.4kDa), crosslinker (10%, 20% 4-arm PEG acrylate), and polymer concentration (3.6, 7.2, 10, 20, 30%), in an attempt to identify a correlation between gel mechanical properties and suture-induced damage. Despite the broad range of tensile properties, hydrogel particulates were detected in all PEGDA hydrogels when a suture needle was passed through the hydrogel slabs, Figure 3A. There was no discernable trend between suture-induced damage and compressive modulus, tensile modulus, tensile strength, or elongation, Supplementary Figure 1. In contrast, copolymerization with NVP resulted in a marked decrease in the total number of dislodged particles in all compositions of PEGDA hydrogels tested, Figure 3B. Additional mechanical testing of fracture toughness using a single edge notch tensile test identified a marked increase in fracture toughness in PEGDA-NVP hydrogels (Figure 3C). The force required to propagate the notch across the hydrogel was increased for all PEGDA-NVP compositions and correlated strongly with decreased suture-induced damage as measured by particle generation (Figure 3D).

Effect of NVP concentration in PEGDA gels

The effect of NVP concentration on the suture damage and compressive modulus of the PEGDA gels was tested (Figure 4). The number of dislodged hydrogel particles decreased as increasing amounts of NVP were incorporated with particles ultimately eliminated with 54 moles of NVP added to the precursor solution for every 1 mole of PEGDA in solution, Figure 4A. A concurrent increase in compressive modulus of the 10% PEG(3.4k)DA hydrogels was observed with increasing amounts of NVP, Figure 4B. In order to match the original compressive modulus, the polymer content was decreased to 7.2% PEG(3.4k)DA-NVP 1:54, which resulted in a corollary decrease in compressive modulus to approximately 470 kPa (Figure 4C).

Evaluation of PEGDAA-NVP hydrogel as a candidate luminal layer

Following identification of a method to enhance resistance to suturing damage of PEG-based hydrogels, additional testing was performed to identify and evaluate a candidate hydrogel composition for use as the luminal layer of the multilayer grafts. Previous studies have demonstrated favorable cell adhesion and migration on the 10% PEG(3.4k)DA hydrogels and enhanced hydrolytic stability of PEGDAA hydrogels.[6, 7, 12] In an effort to match the physical properties and biostability of these previous compositions, a new 7.2% PEG(3.4kDa)DAA-NVP was fabricated and tested in comparison to the 10% PEG(3.4kDa)DA hydrogel. The PEGDAA-NVP formulation displayed comparable compressive modulus and swelling as the PEGDA control with an increase in defect tolerance as indicated by the elimination of suture-induced particles generation, Figure 5. Biostability of the PEGDAA-NVP was then assessed using accelerated hydrolytic testing. No significant difference in the equilibrium swelling ratio of the PEGDAA-NVP hydrogel was observed; whereas, the PEGDA hydrogels were fully degraded at 5 days.

Thromboresistance is another critical property to the success of any blood contacting material and was previously established in the original PEGDA hydrogel coating.[5] As an initial assessment that thromboresistance was retained in the new composition, static platelet attachment was assessed on PEGDAA-NVP hydrogel slabs. A synthetic graft, ePTFE, served as a clinical control and displayed significant platelet attachment, 10.3 ± 4.9 platelets/cm². In contrast, a statistically significant decrease in platelet attachment was measured on both the original PEGDA (1.5 ± 1.3 platelets/cm²) or new PEGDAA-NVP (0.47 ± 0.49 platelets/cm²) hydrogels. There was no significant difference between the PEGDA or PEGDAA-NVP suggesting that altering the hydrogel formulation to improve defect tolerance had limited impact on platelet attachment.

Finally, the ability to confer bioactivity to the PEGDAA-NVP hydrogels was evaluated by incorporating acrylate-functionalized collagen and assessing endothelial cell adhesion. BAEC attachment studies demonstrated a statistically significant increase in cell attachment and cell spreading with collagen incorporated compared to the hydrogel controls. No significant differences were measured between PEGDA or PEGDA-NVP hydrogel compositions in either number of cells adhered (100 ± 6 cells/mm² and 94 ± 6 cells/mm²) or cell spreading (942 ± 22 μ m/cell and 762 ± 35 μ m/cell), respectively (Figure 6). Following these favorable results, this composition was selected for the luminal layer of the multilayer vascular graft.

Evaluation of the multilayer vascular graft

Multilayer vascular grafts were fabricated with the new defect-tolerant hydrogel composition (7.2% PEG(3.4kDa)DAA-NVP) and grafts were evaluated for biostability, thromboresistance, and suture-induced damage in comparison to the previous hydrogel composition (10% PEG(3.4 kDa)).[5] In order to assess the effects of hydrogel degradation and subsequent swelling on the hydrogel luminal layer, accelerated hydrolytic degradation was performed on composite grafts with either PEGDA or PEGDAA-NVP inner layers. The PEGDA luminal diameter decreased by the first day, and continued to decrease until eventually the PEGDA inner layer delaminated from the outer layer and achieved total

dissolution by day 5. The PEGDAA-NVP inner layer demonstrated no change in the luminal diameter over the course of 28 days (Figure 7B).

Given the low platelet attachment on hydrogels under static conditions described above (Figure 8A), the multilayer vascular grafts were assessed with whole blood in a pulsatile flow bioreactor. The results of the whole blood attachment studies closely mirror the trends in the platelet attachment study. Low platelet attachment on the PEGDA (0.08 ± 0.02 platelets/cm²) and PEGDA-NVP (0.1 ± 0.05 platelets/cm²) composites was observed and the results were statistically different than platelet attachment on the ePTFE graft (0.5 ± 0.2 platelets/cm²), Figures 8B and 8C.

Finally, an *ex vivo* flow loop model was used to provide a more rigorous simulation of the implantation procedure and assess particle generation following suturing of the multilayer grafts, Figure 9A. The number of dislodged hydrogel particles were counted in both the storage solutions of the sutured grafts and the solutions collected from the flow loop set up. Particulates were identified in all solutions except the sham control. More hydrogel particulates were identified in the storage containers of both formulations than in the flow solutions. There was also a statistically significant increase in particles detected in the solutions of the PEGDA composition than in the PEGDAA-NVP composition, Figure 9B. Upon investigation of the sutured ends of the grafts, the hydrogel layer of the PEGDAA-NVP composites appeared intact; whereas, marked damage to the hydrogel layer of the PEGDA composites was noted at the suture line, Figure 9C. Additional analysis of the graft indicated damage to the center of both sets of grafts and attributed to forceps gripping of the graft during the suturing procedure. Composite grafts with thinner hydrogel luminal wall thickness did not display this compressive damage, Supplemental Figure 2.

DISCUSSION

The observed suture-induced damage of the hydrogel coating after implantation of the multilayer vascular graft created a clear need for a hydrogel with increased defect tolerance. Hydrogel particulates from suture-induced damage can result in embolisms downstream leading to severe complications and morbidity. To generate a new hydrogel coating that could be used clinically without risk of embolism, traditional hydrogel variables (molecular weight, concentration, crosslinker) were investigated to first identify a correlation between gel mechanical properties and suture-induced particle generation. Despite the large ranges investigated for modulus (6 kPa to 66 kPa), tensile strength (11 kPa to 43 kPa), and elongation (7% to 314%), no strong correlation was observed between these properties and suture damage resistance (Supplemental Figure 1). The mechanical property that could be correlated with defect tolerance was fracture toughness as measured by a single edge notch test. The energy required for crack propagation was a better predictor of hydrogel defect tolerance and particle generation during suturing. Increased fracture toughness was achieved in the PEG-based hydrogels through copolymerization with NVP and attributed to the additional hydrogen bonding sites available upon NVP incorporation. Although there are several possible secondary interactions, one such is water bridging between the carbonyl of the NVP amide and the carbonyls of the ester of PEGDA or amide of PEGDAA, as diagrammed in Figure 10. It has been demonstrated that an increase in secondary force

interactions between polymer chains requires greater energy to initiate crack propagation, and this higher initiation energy creates a higher defect tolerance in the crosslinked polymer. [9, 13] For our system, the addition of NVP to the PEG-based hydrogels was hypothesized to reduce suture-induced damage by introducing sacrificial, hydrogen bonds that dissipate initial crack energy and potentially reform to limit future crack propagation and fracture.

In order to achieve incorporation and total elimination of dislodged hydrogel particulates, relatively large amounts of NVP (54 moles to 1 mole of PEGDA) must be added to the hydrogel precursor solution. During formation of the crosslinked hydrogel network, three simultaneous reactions take place upon UV irradiation of the pre-cursor solution: homopolymerization of the acrylates in PEGDA, homopolymerization of the vinyls in NVP, and copolymerization of the acrylates and vinyls. According to an assay for the detection of tertiary amines developed by El-Rabbat et al., approximately $16 \pm 9\%$ of the NVP added is incorporated into the hydrogel network. The high sol fraction (Supplemental Figure 3) also supported a low level of NVP incorporation into the network. This result is expected given that the propagation rate (k_p) is much higher for acrylate-acrylate reactions (2.165×10^4 L/mol-s) than for acrylate-vinyl reactions (0.101×10^4 L/mol-s). This strongly favors polymerization of the PEGDA over copolymerization of PEGDA and NVP due to the limited availability of the acrylate groups for reaction. Therefore, large molar ratios of NVP to PEGDA must be added in order for NVP to be incorporated.

Although increasing amounts of NVP increased defect tolerance, it also increased the compressive modulus of the resulting hydrogel, Figure 4. It was hypothesized that the increase in compressive modulus and decrease in swelling ratio was due to an overall increase in polymer concentration in the final gel and corollary decrease in mesh size. However, when overall polymer content (PEGDA and NVP) is kept constant, there is a decrease in compressive modulus and increase in swelling, likely due to the disruption of network formation by NVP, Supplemental Table 1. Based on this finding, modulus was reduced to match the PEGDA control by decreasing the PEGDA concentration of the hydrogel. The resulting hydrogel maintained a similar defect tolerance and similar swelling ratio as the PEGDA hydrogel control. This suggests that the hydrogels mechanical properties can be tailored without altering suture damage resistance, Figure 5.

In addition to suture damage resistance, it is important the hydrogel coating is resistant to hydrolytic degradation to ensure it remains intact for the lifetime of the graft. In order to accomplish this, the formulation was changed from a PEGDA based hydrogel that contains ester linkages to PEGDAA that contains more hydrolytically stable amide linkages. Previous work in our lab has demonstrated the *in vitro* and *in vivo* hydrolytic stability of the PEGDAA hydrogels.[12] The PEGDAA-NVP displayed a similar resistance to hydrolysis as evidenced by the accelerated hydrolytic degradation study. Stability of the graft inner layer is critical to supporting the endothelial cell layer as well as preventing occlusion of the graft due to increased swelling of the hydrogel, Figure 7.

Following confirmation that the defect-tolerant hydrogel formulation maintained bioactivity and thromboresistance, a preliminary ex vivo suturing study was performed by suturing the composite graft to excised porcine carotid arteries. Preventing hydrogel damage is critical to

the clinical relevance of the multilayered graft, as dislodged hydrogel particulates can act as emboli in the vascular system, and cause downstream heart attacks and strokes. This study demonstrated that significantly fewer particles are dislodged from the PEGDAA-NVP hydrogel coated graft than from the PEGDA hydrogel coated graft, Figure 9. Upon investigation of the suture line, the PEGDAA-NVP hydrogel appeared intact whereas the PEGDA hydrogel displayed severe damage, Figure 1C. The dislodged particles in the PEGDAA-NVP hydrogel detected in the storage solutions were attributed to damage of the hydrogel layer at the middle of the graft due to gripping with forceps to stabilize the graft during suturing (Supplemental Figure 2). We have confirmed that the gripping damage can be mitigated by using thinner hydrogel coatings in the graft composites. This eliminates all dislodged particles, making the coating efficacious for clinical application.

CONCLUSIONS

Our previous work developing small diameter vascular grafts led to the discovery of the unique problem of particles dislodged from the hydrogel luminal layer during suturing. To address this problem, a new PEGDAA-NVP hydrogel with improved fracture toughness was developed. Increased defect tolerance was achieved through the introduction of sacrificial, hydrogen bonds that enabled suturing of the multilayer vascular graft without particle generation. It was also demonstrated that this modification resulted in no significant increase in thrombogenicity or change in bioactivity compared to a well-characterized PEGDA hydrogel. Therefore, we have successfully addressed the need for a suture-damage resistant hydrogel coating for use in small diameter vascular grafts and highlighted the need for testing the generation of dislodged particles in blood contacting materials. Future work will build upon the current research by testing the initial thromboresistance and long-term stability of the multilayered vascular graft with the new hydrogel inner layer after implantation into a porcine carotid artery model.

Supplementary Material

Refer to Web version on PubMed Central for supplementary material.

Acknowledgments

The work presented here was supported by the Texas A&M University Diversity Fellowship and the National Institutes of Health R21 EB020978-01 and R01 EB013297. The Bionate® Thermoplastic Polycarbonate-urethane was provided by DSM Biomedical (Berkeley, CA).

References

1. Salacinski HJ, Goldner S, Giudiceandrea A, Hamilton G, Seifalian AM, Edwards A, Carson RJ. The mechanical behavior of vascular grafts: a review. *Journal of biomaterials applications*. 2001; 15:241–78. [PubMed: 11261602]
2. Sarkar S, Sales KM, Hamilton G, Seifalian AM. Addressing thrombogenicity in vascular graft construction. *Journal of Biomedical Materials Research Part B: Applied Biomaterials*. 2007; 82:100–8.
3. Rabkin E, Schoen FJ. Cardiovascular tissue engineering. *Cardiovascular Pathology*. 2002; 11:305–17. [PubMed: 12459430]

4. Ratcliffe A. Tissue engineering of vascular grafts. *Matrix Biology*. 2000; 19:353–7. [PubMed: 10963996]
5. Browning M, Dempsey D, Guiza V, Becerra S, Rivera J, Russell B, Hook M, Clubb F, Miller M, Fossum T. Multilayer vascular grafts based on collagen-mimetic proteins. *Acta biomaterialia*. 2012; 8:1010–21. [PubMed: 22142564]
6. Browning MB, Guiza V, Russell B, Rivera J, Cereceres S, Höök M, Hahn MS, Cosgriff-Hernandez EM. Endothelial cell response to chemical, biological, and physical cues in bioactive hydrogels. *Tissue Engineering Part A*. 2014; 20:3130–41. [PubMed: 24935249]
7. Browning MB, Russell B, Ri, Cosgriff-Hernandez EM. Bioactive hydrogels with enhanced initial and sustained cell interactions. *Biomacromolecules*. 2013; 14:2225–33. [PubMed: 23758437]
8. Jaff MR, McMurtry MS, Archer SL, Cushman M, Goldenberg N, Goldhaber SZ, Jenkins JS, Kline JA, Michaels AD, Thistlethwaite P, Vedentham S, White RJ, Zierler BR. Management of Massive and Submassive Pulmonary Embolism, Iliofemoral Deep Vein Thrombosis, and Chronic Thromboembolic Pulmonary Hypertension. A Scientific Statement From the American Heart Association. 2011; 123:1788–830.
9. Myllymäki TTT, Lemetti L, Nonappa, Ikkala O. Hierarchical Supramolecular Cross-Linking of Polymers for Biomimetic Fracture Energy Dissipating Sacrificial Bonds and Defect Tolerance under Mechanical Loading. *ACS Macro Letters*. 2017; 6:210–4.
10. Hahn MS, Taite LJ, Moon JJ, Rowland MC, Ruffino KA, West JL. Photolithographic patterning of polyethylene glycol hydrogels. *Biomaterials*. 2006; 27:2519–24. [PubMed: 16375965]
11. El-Rabbat N, Askal HF, Khashaba PY, Attia NN. A validated spectrofluorometric assay for the determination of certain macrolide antibiotics in pharmaceutical formulations and spiked biological fluids. *Journal of AOAC International*. 2006; 89:1276–87. [PubMed: 17042176]
12. Browning MB, Cosgriff-Hernandez E. Development of a Biostable Replacement for PEGDA Hydrogels. *Biomacromolecules*. 2012; 13:779–86. [PubMed: 22324325]
13. Nakajima T. Generalization of the sacrificial bond principle for gel and elastomer toughening. *Polym J*. 2017

STATEMENT OF SIGNIFICANCE

Small-caliber vascular grafts used in coronary artery bypass procedures typically fail due to development of intimal hyperplasia or thrombosis. Our laboratory has developed a multilayered vascular graft with an electrospun polyurethane outer layer with improved compliance matching and a hydrogel inner layer that is both thromboresistant and promotes endothelialization. However, hydrogel particulates were dislodged from the hydrogel layer during suturing *in vivo*. This work describes a hydrogel formulation based on poly(ethylene glycol) that is resistant to suture-induced damage. The introduction of sacrificial, hydrogen bonds by co-polymerization with n-vinyl pyrrolidone (NVP) resulted in an increase fracture energy without affecting the thromboresistance, bioactivity, or biostability. This defect-tolerant hydrogel formulation and the methodology to assess hydrogel defect tolerance has broad potential use in cardiovascular and soft tissue applications.

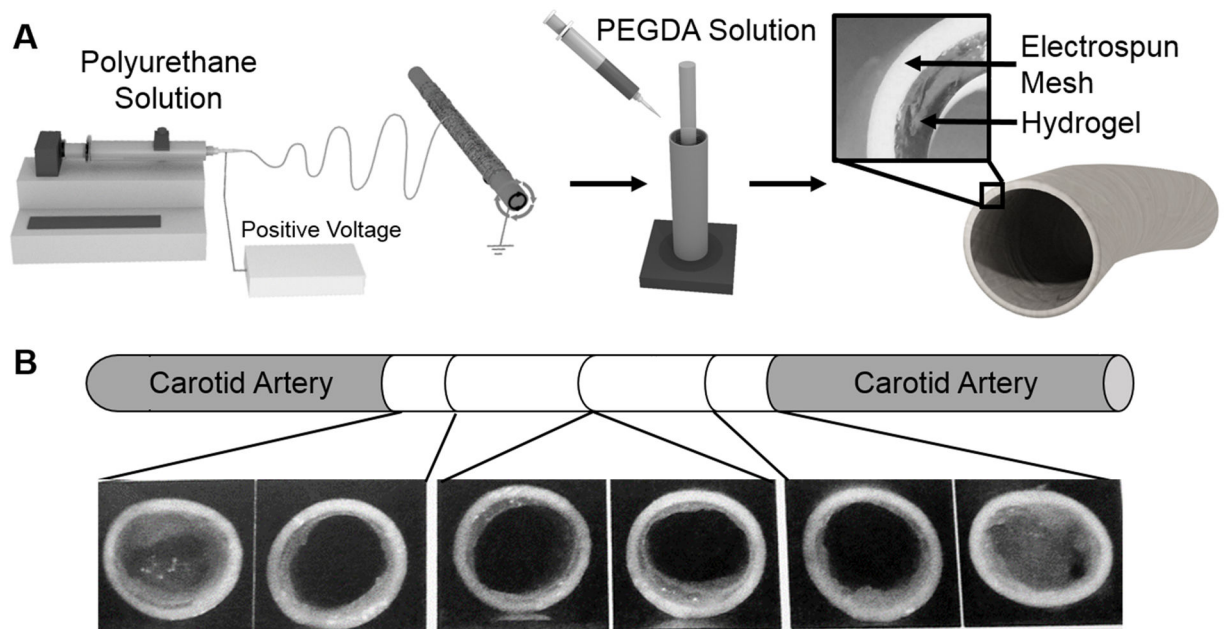


Figure 1.

A) Schematic of multilayer graft fabrication. B) Damage of the hydrogel at the suture line of multilayer graft composites implanted in porcine animal model.

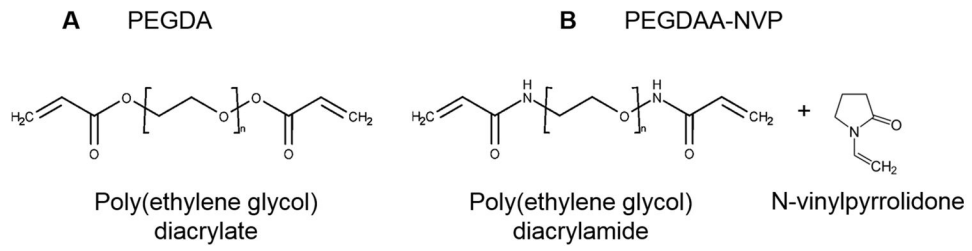


Figure 2. Chemical structures of A) poly(ethylene glycol) diacrylate (PEGDA) with an ester linkage, and of B) poly(ethylene glycol) diacrylamide (PEGDAA) with an amide linkage and n-vinylpyrrolidone (NVP).

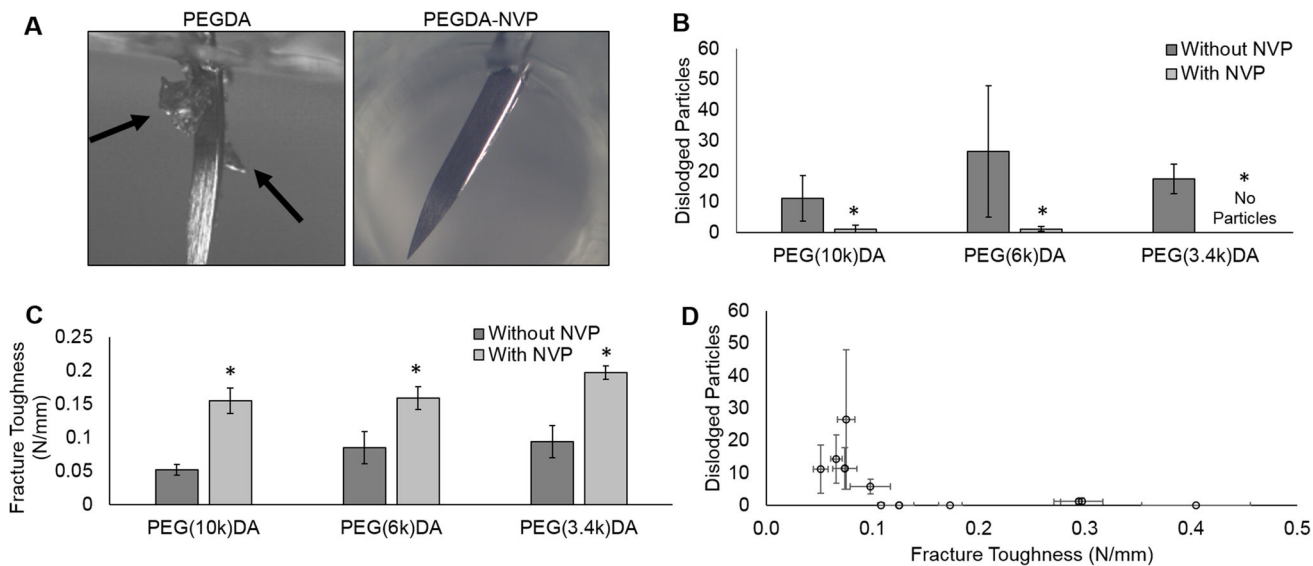


Figure 3. A) Images of particles dislodged during suturing for both PEG(3.4k)DA and PEG(3.4k)DA-NVP hydrogel compositions. Black arrows indicate dislodged particles. B) Effect of incorporating NVP into 10% PEGDA hydrogels on suture damage resistance. C) Defect tolerance assessed by fracture toughness. D) Correlation of reduced particle generation during suturing with increasing fracture toughness. All data represents average \pm standard deviation of $n=6$. The * represents a significant difference between groups with and without NVP ($p<0.05$).

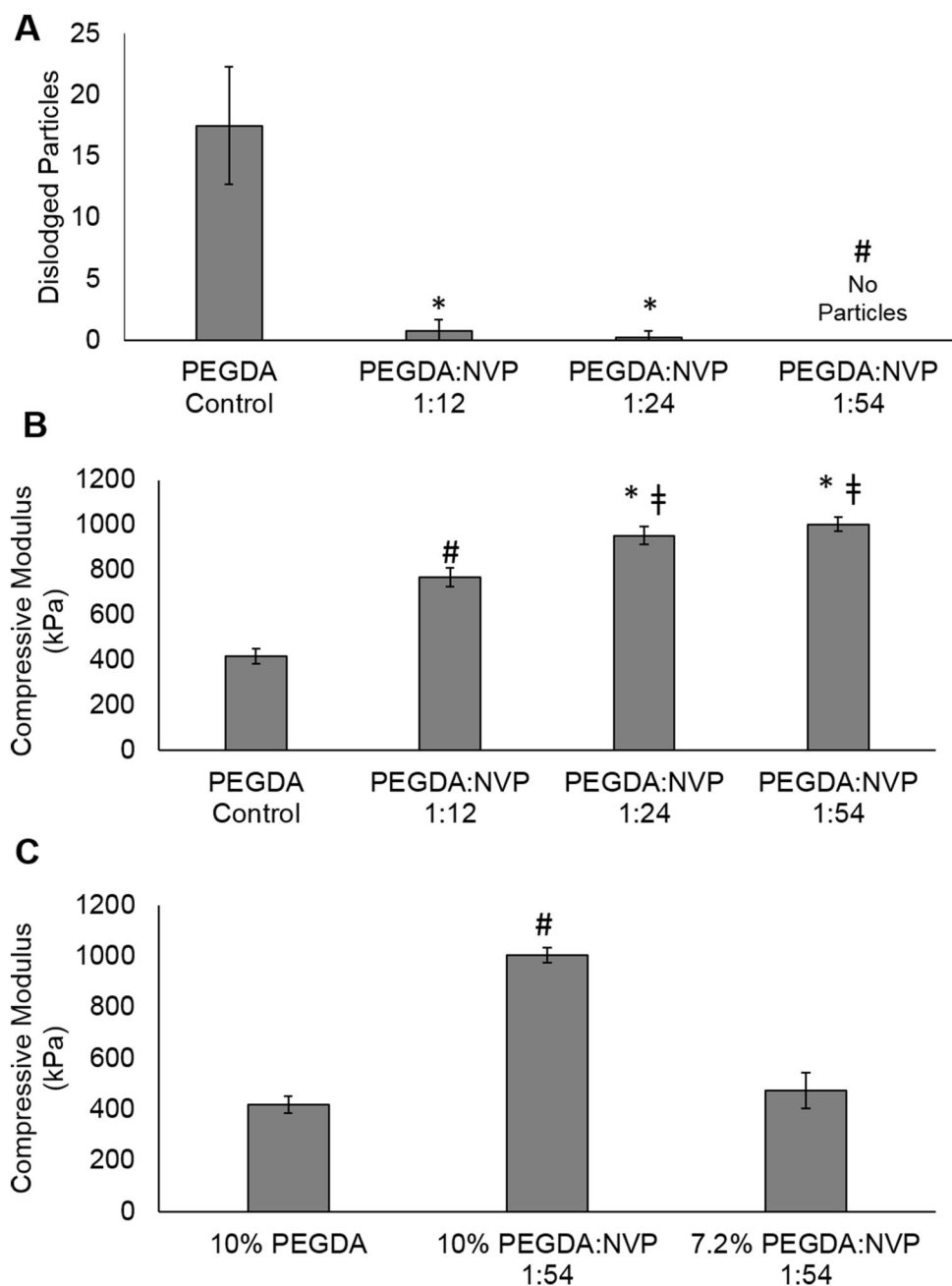


Figure 4.

Effect of increasing NVP content in 10% PEG(3.4k)DA hydrogels on (A) defect tolerance and (B) compressive modulus. (C) Matching modulus of the 10% PEGDA with the PEGDA-NVP formulation by decreasing PEGDA content. Data represents average \pm standard deviation of $n=6$. The * represents a significant difference from the PEGDA Control, the # represents significant difference from the control and PEGDA:NVP 1:12, and the ‡ represents significant difference from all other groups ($p<0.05$) in ANOVA with Tukey's multiple comparison test.

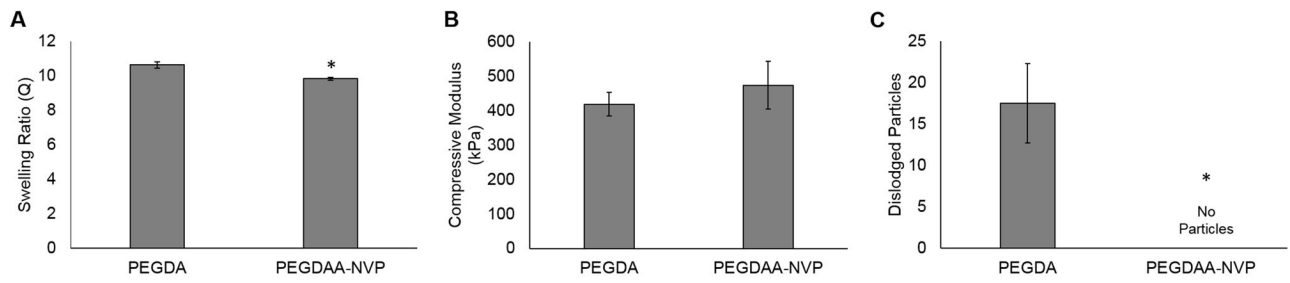


Figure 5. Matching swelling (A) and compressive modulus (B) between the original 10% PEG(3.4k)DA formulation and the damage-resistant 7.2% PEG(3.4k)DAA + 1:54 mol NVP hydrogel. C) Effect of decreasing polymer content and adding NVP to improve the defect tolerance of the hydrogel. Data represents average \pm standard deviation of $n=6$. The * represents a significant difference from PEGDA ($p < 0.05$) in a student's t-test.

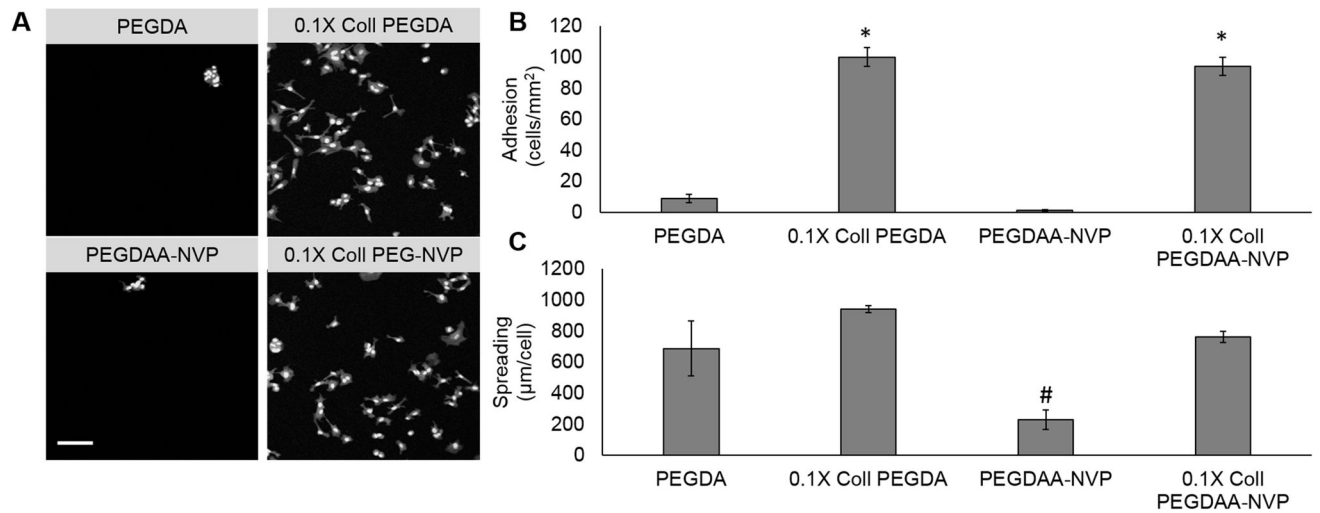


Figure 6.

A) The effect of hydrogel composition on cell adhesion. Scale bar = 100µm. B) BAEC attachment on both compositions with incorporated functionalized collagen. C) BAEC spreading on both compositions with incorporated functionalized collagen. Data represents average \pm standard error of $n=4$. The * represents a difference between groups with and without collagen ($p<0.05$), and the # represents a significant difference from all others ($p<0.05$) in ANOVA with Tukey's multiple comparison test.

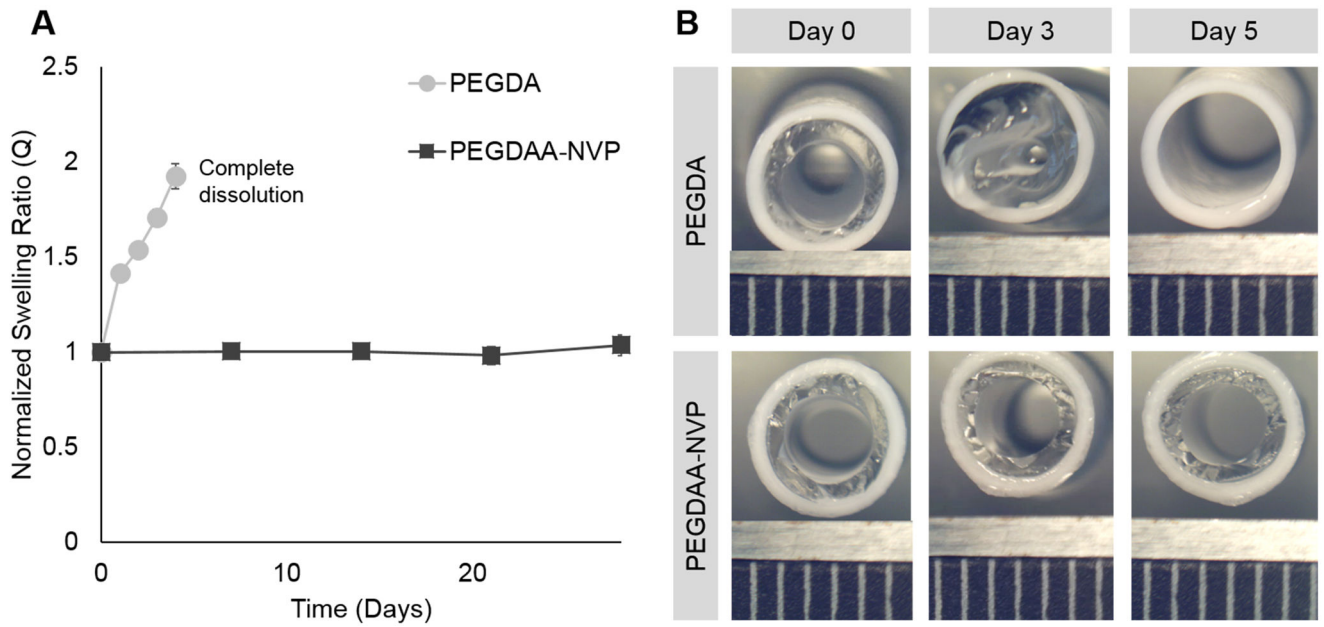


Figure 7. A) The effect of hydrogel composition on hydrolytic degradation rate. B) Luminal diameter changes for both compositions; ruler scale is 1mm. Data represents average \pm standard deviation of n=4.

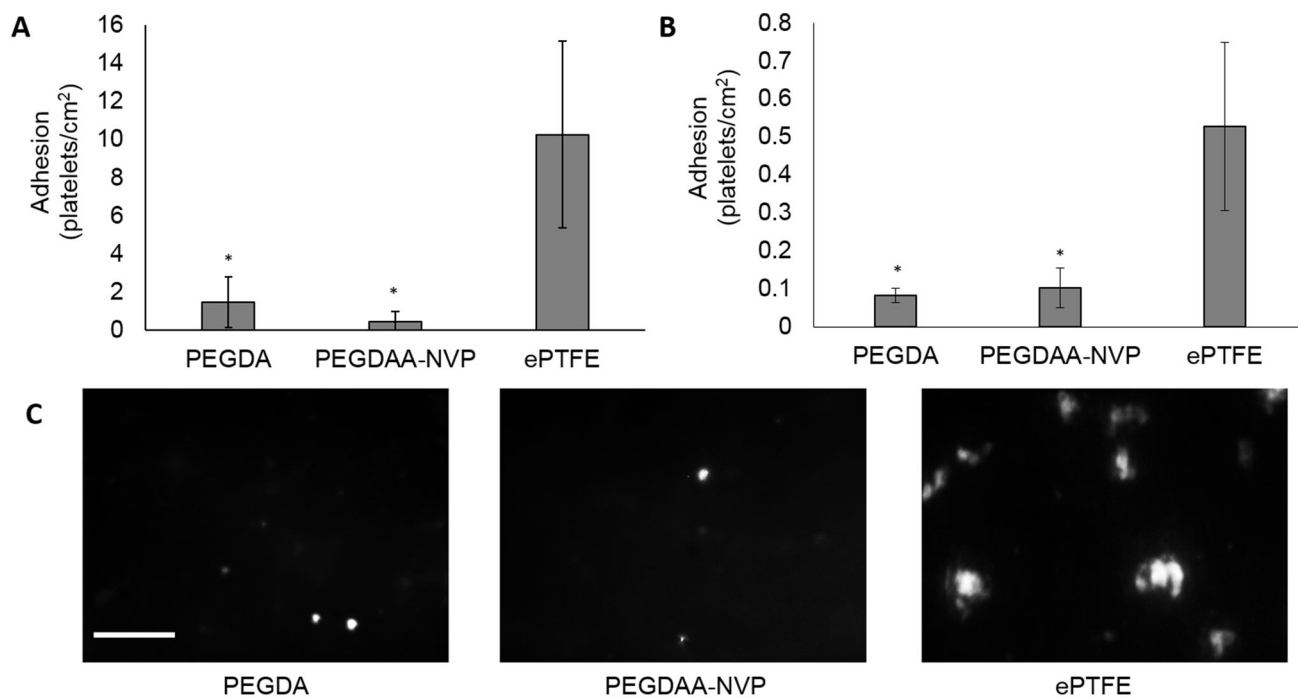


Figure 8.

A) The effects of hydrogel composition on static platelet adhesion. B) The effects of hydrogel composition on bioreactor whole blood platelet attachment. Scale bar = 100 μ m. C) Representative images of platelet attachment from the whole blood study. Data represents average \pm standard deviation of n=4. The * represents a significant difference from ePTFE control ($p < 0.05$) in ANOVA with Tukey's multiple comparison test.

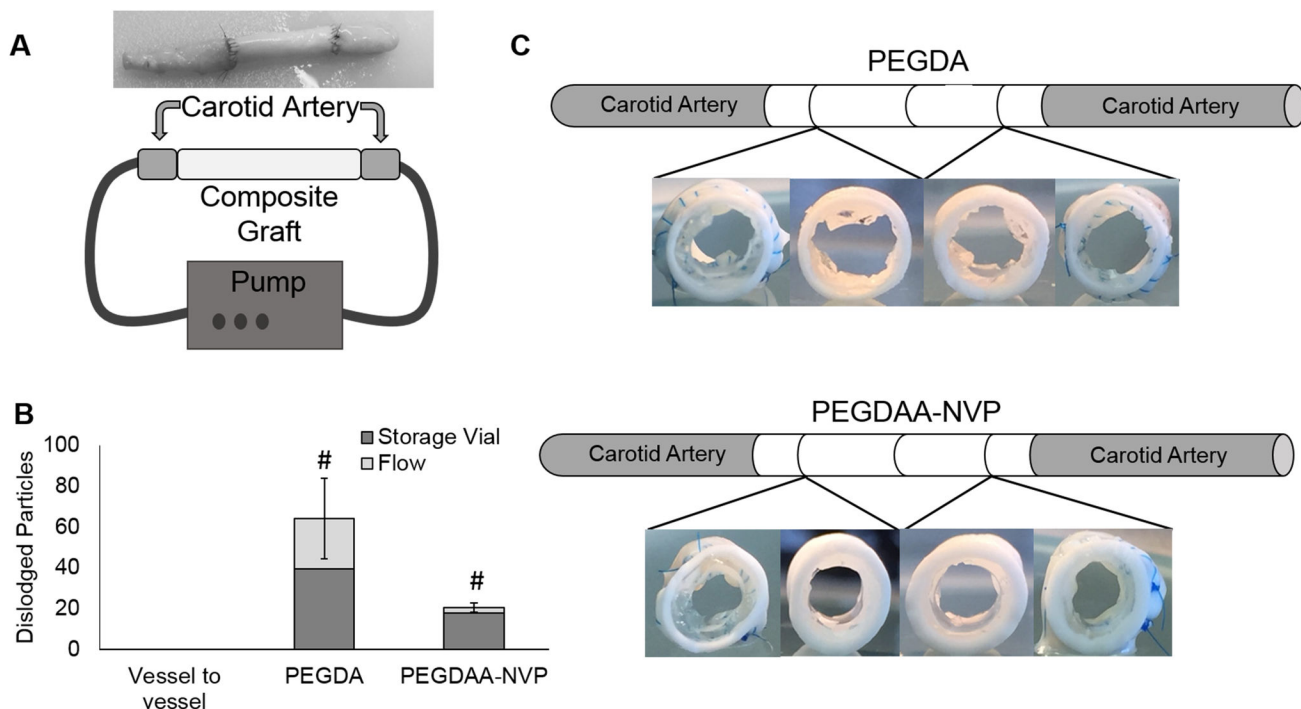


Figure 9. A) Composite graft sutured to excised porcine carotid artery segments and diagram of flow loop. B) Effect of composition on the number of particles captured in the flow loop after in vitro suturing. C) Sectioned grafts demonstrating hydrogel suture line damage after in vitro suturing. Data represents average \pm standard deviation of n=4. The # represents a difference from all others ($p < 0.05$) in ANOVA with Tukey’s multiple comparison test.

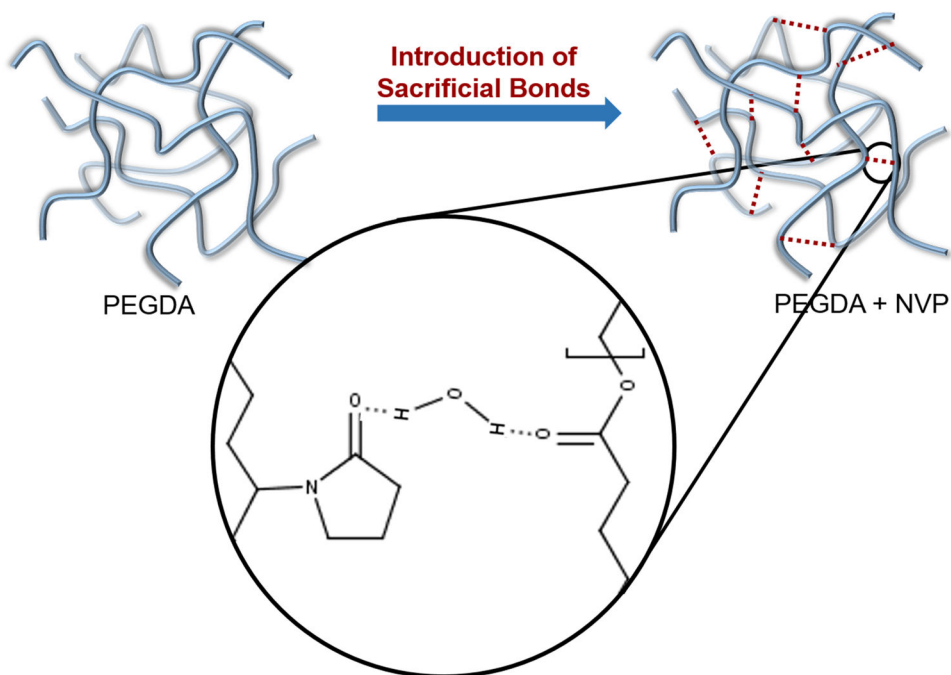


Figure 10.

The effect of adding n-vinyl pyrrolidone to PEGDA hydrogels on defect tolerance. Fracture energy is increased by introducing sacrificial bonds via increased hydrogen bonding, thereby increasing defect tolerance. The sacrificial hydrogen bonds are created by water bridging of the carbonyl of the PEGDA ester and the carbonyl of the NVP amide groups.